13th World Conference on Earthquake Engineering
Vancouver, B.C., Canada
August 1-6, 2004
Paper No. 1556

IMPROVING PROBABILISTIC SEISMIC DEMAND MODELS THROUGH REFINED INTENSITY MEASURES

Kevin MACKIE[1]
Bozidar STOJADINOVIC[2]

SUMMARY

In the Pacific Earthquake Engineering Research Center's probabilistic performance-based earthquake engineering framework, determining the probability of achieving a performance objective is de-aggregated into several interim models. One fundamental building block is the probabilistic seismic demand model (PSDM), which relates measures of earthquake intensity to measures of structural response. An optimal demand model is one that has a clearly defined mathematical form and exhibits low uncertainty. Lower uncertainty allows a higher level of confidence among the comparable demand models, which subsequently leads to higher confidence in the probability of achieving the desired performance objectives.

Three classes of intensity measures (IMs) are used in current practice. The first class contains traditional IMs that describe the earthquake source characteristics and time history record. The second class involves the IMs that describe the time history obtained using a single-degree-of-freedom system filter on the original record. The third class extends this concept to IMs that result from applying an arbitrary filter to the original time history. Reducing the uncertainty can be achieved by using more refined intensity measures containing more information about the structure of interest in the demand model. Traditionally, more information is introduced by combining IMs belonging to the second IM class. However, it is also possible to introduce more information about the structure by using other more sophisticated structure-related filters and judicious selection of input parameters to those filters.

This paper addresses improvement in PSDMs through selection of input parameters to the second class of IMs and the use of new filters to the third class. A parametric study is accomplished using probabilistic seismic demand models derived for single-column bent reinforced concrete highway overpass bridges that cover a wide range of typical bridge designs in California. In particular, optimal selection of input parameters, such as damping and inelastic yielding criteria, is presented. A set of IMs and corresponding structure-related filters are recommended such that they produce optimal demand models with low uncertainty.

[1] PhD candidate, University of California Berkeley, USA. Email: mackie@ce.berkeley.edu
[2] Associate Professor, University of California Berkeley, USA. Email: boza@ce.berkeley.edu

INTRODUCTION

Performance-based earthquake engineering (PBEE) describes a quantitative means for designers of structures to achieve predetermined performance levels or objectives in a specific hazard environment. Among the recent implementations of PBEE, the Pacific Earthquake Engineering Research Center (PEER) is developing a probabilistic framework for performance-based design and evaluation. It allows for a complete probabilistic evaluation of the PBEE problem by de-aggregating the ultimate performance objective into interim models and objectives. A brief description of the process is described below. See Krawinkler [1] and Cornell [2] or a more rigorous treatment. Performance objectives are defined in terms of annual probabilities of socio-economic Decision Variables (DV) being exceeded in a seismic hazard environment. The DVs are then conditioned on global or component Damage Measures (DM), such as concrete spalling. These DMs are then conditioned on Engineering Demand Parameters (EDP), measures of structural performance such as interstory drift ratio. These EDPs are usually obtained from nonlinear analysis using different ground motions, described in terms of seismic hazard Intensity Measures (IM).

The uncertainties over the full range of model variables are systematically addressed and propagated, making the selection of each interim model critical to the process. This paper addresses only the interim demand model, or the relation between structural demand and earthquake intensity. Probabilistic Seismic Demand Analysis (PSDA) is done in order to estimate the mean annual frequency (ν) of exceeding a given structural engineering demand measure ($EDP > y$) in a given hazard environment ($IM = x$), as detailed in Equation 1.

$$\nu_{EDP}(y) = \int_x P_{EDP|IM}(y \mid x) \left| d\nu_{IM}(x) \right| dx \tag{1}$$

The conditional probability term in Equation 1 is referred to as a Probabilistic Seismic Demand Model (PSDM), and minimizing it's associated uncertainty is the subject of this paper. Besides uncertainty, there are other criteria for judging a demand model. One that meets all of these criteria is deemed optimal.

Optimal is defined as being practical, sufficient, effective, efficient, and robust [3]. An IM-EDP pair is practical if it has some direct correlation to known engineering quantities. Sufficiency describes whether the IM-EDP pair has a conditional dependence on ground motion characteristics, such as magnitude and distance. These two issues are not addressed in this paper, and should be verified separately. For example, see Cornell [4]. Effectiveness of a demand model is determined by the ability to fit a mathematical form to the median trend. For this to be accomplished, it is assumed the EDPs follow a lognormal distribution [5]. Thus a relation describing the median demand model can be written as Equation 2.

$$\hat{EDP} = a(IM)^b \tag{2}$$

The models were not evaluated for effectiveness explicitly, but better IMs were chosen based on dispersion values that were derived from minimizing the scatter about a linear (in log space) fit. Therefore all of the optimal models are implicitly effective.

Efficiency is the amount of variability (randomness) of an EDP given an IM surrounding the exponential fit. The measure used to evaluate efficiency is the dispersion, defined as the standard deviation of the logarithm of the demand model residuals [5]. An efficient demand model requires a smaller number of nonlinear time-history analyses to achieve a desired level of confidence. Therefore by minimizing the dispersion, tighter confidence bands on resulting demand, and ultimately decision, performance objectives can be achieved. For example, lowering the dispersion by a factor of two would require four times fewer ground motion records [12] to achieve the same confidence interval. Robustness describes the rate of change of efficiency with period. An IM with a small rate of change is deemed robust.

The demand models in this paper were formulated using a standard PSDA procedure [3]. The details of the ground motions used, the model, and analysis methods are discussed in detail previously by Mackie [3, 6]. The PSDA method uses a cloud of ground motions to generate the PSDM. Alternatively, the EDP distribution at a particular IM can be determined by stripe analysis [12]. There are two primary caveats to using the cloud procedure as opposed to stripe analysis. First, the dispersion includes not only the randomness inherent in ground motions, but also a contribution from the error due to the choice of regression form over an IM range. Therefore, the total error might be overestimated due to this model error. Second, the dispersion is assumed constant over the entire IM range, an assumption that is often false at high intensities. However, for the purposes of this study, the standard PSDA approach is acceptable, as the IM range does not include extremely high intensities and a treatment of collapse. Additionally, as mentioned above, highly efficient models are implicitly effective, and as the dispersion is reduced, so is the model error. The dispersion is used solely as a means for comparing multiple IMs, therefore determining the proportion of model error in each is less important.

The class of structures considered is typical new California highway overpass bridges designed according to Caltrans SDC [7]. Specifically, only single-bent, single-column-per-bent reinforced concrete bridges were considered. Bridges are all assumed to be of newer, and hence ductile, construction. Individual bridge designs were created by choosing values from a set of design parameters. These include span length, column diameter, column height, material strengths, soil stiffness, superstructure weight, etc. All bridge models were fully three-dimensional and included earthquake excitation in all three principal directions.

A subset of the bridges was used in this study to evaluate such issues as the efficiency dependence on structural period. The bridges used, their design parameters, and lowest longitudinal and transverse periods are presented in Table 1. The periods designated with "pre" refer to the initial elastic periods, while those designated "post" refer to the elastic period after gravity load equilibrium. To be strictly accurate, there is only one fundamental period (the lowest period) per structure; however, the earthquake response of the structure is considered separately in the longitudinal and transverse directions. The mode shapes also exhibit deformation in each direction exclusively. Therefore, the lowest period corresponding to each of those directions is shown in Table 1. This notation is adopted because, in the post-gravity load analysis case, the longitudinally dominated mode may be mode 1, 2, or 3.

Table 1 - Summary of bridges and structural periods

Structure number	L/H	Dc/Ds	$T_{1,long}$ pre	$T_{1,tran}$ pre	$T_{1,long}$ post	$T_{1,tran}$ post
0001	2.4	0.75	1.40	1.57	1.45	2.09
0005	3.5	0.75	1.15	1.31	1.19	2.03
0009	1.8	0.75	1.76	1.94	1.82	2.20
0013	1.2	0.75	2.54	2.74	2.64	2.94
0017	2.4	0.67	1.63	1.77	1.69	2.18
0021	2.4	1.00	0.98	1.23	1.03	1.98
0025	2.4	1.30	0.76	1.08	0.78	1.58

An important distinction, however, is the fundamental period is always used when forming any structure dependent demand models. The issue of period is resolved further in the parameter study. For all of the efficiency and robustness plots shown, the longitudinal demand model has been utilized, unless otherwise noted. It is also, therefore, implied the same conclusions can be drawn about the performance of IMs in a transverse demand model. Drift ratio is the global EDP used herein and is not mentioned explicitly from

this point on. The same methodology can be applied to evaluation of IM performance with non-global EDPs such as maximum column moment, but results are not discussed in this paper. Discussion of the applicability of the results in this paper to other EDPs is included in the conclusion.

The range of bridge periods considered was purposely selected to be in the medium to long period, or the constant velocity spectral regime. This was done to avoid drawing conclusions about the efficiency of IMs that are better predictors for short period structures, such as *PGA* and I_A. However, it does suggest IMs such as *PGV* and *PGD* would be more efficient in this period range. The optimal IM is robust across a large period range; therefore, it is mentioned when an IM in this study is only effective over particular period ranges.

This paper specifically addresses the computation of IMs that can be obtained directly from time history records (because Class I IMs were applied to all filtered records). It should be noted then that other IMs and ground motion descriptors do exist that are not covered by this procedure. These include magnitude, frequency content measures such as Fourier amplitude, and iterative measures such as F_μ developed by Conte [8].

CLASS I INTENSITY MEASURES

Class I Intensity Measures are defined as those that can be generated directly from the recorded earthquake time history (from time t=0 to time t=D, the record duration). Time history information is usually presented in acceleration units, therefore, integration of the time history to obtain velocity and displacement histories may also be necessary. Procedures for correct record integration are outlined in Joyner and Boore [9]. In this study, seventeen Class I IMs were considered. These are summarized in Table 2, with their associated IM number in this study. Note that not all IM numbers in forthcoming tables are consecutive. The range of IM numbers is enumerated within each IM class.

Table 2 - Class I Intensity Measure Definitions

IM number	IM name	Definition	Units
1	Strong motion duration	$T_D = t(0.95 I_A) - t(0.05 I_A)$	s
2	Peak ground acceleration	$PGA = \max\left\|\ddot{u}_g(t)\right\|$	g
3	Peak ground velocity	$PGV = \max\left\|\dot{u}_g(t)\right\|$	cm/s
4	Peak ground displacement	$PGD = \max\left\|u_g(t)\right\|$	cm
5	Arias intensity [10]	$I_A = \frac{\pi}{2g}\int_0^D \left[\ddot{u}_g(t)\right]^2 dt$	cm/s
6	Velocity intensity	$I_V = \frac{1}{PGV}\int_0^D \left[\dot{u}_g(t)\right]^2 dt$	cm
7	Displacement intensity	$I_D = \frac{1}{PGD}\int_0^D \left[u_g(t)\right]^2 dt$	cm-s
8	Cumulative absolute velocity	$CAV = \int_0^D \left\|\ddot{u}_g(t)\right\| dt$	cm/s

9	Cumulative absolute displacement	$CAD = \int_0^D \left\|\dot{u}_g(t)\right\| dt$	cm
10	Cumulative absolute impulse	$CAI = \int_0^D \left\|u_g(t)\right\| dt$	cm-s
11	Root mean square acceleration	$A_{rms} = \sqrt{\frac{1}{T_D}\int_0^D \left[\ddot{u}_g(t)\right]^2 dt}$	cm/s^2
12	Root mean square velocity	$V_{rms} = \sqrt{\frac{1}{T_D}\int_0^D \left[\dot{u}_g(t)\right]^2 dt}$	cm/s
13	Root mean square displacement	$D_{rms} = \sqrt{\frac{1}{T_D}\int_0^D \left[u_g(t)\right]^2 dt}$	cm
14	Characteristic intensity	$I_C = A_{rms}^{1.5} T_D^{0.5}$	cm$^{1.5}$/s$^{2.5}$
15	Frequency ratio 1	$FR_1 = \frac{PGV}{PGA}$	s
16	Frequency ratio 2	$FR_2 = \frac{PGD}{PGV}$	s
17	Medium period IM [11]	$I = PGV\left(T_D^{0.25}\right)$	cm/s$^{0.75}$

The efficiency, measured in terms of dispersion, of all Table 2 IMs is plotted in Figure 1 for several choices of structural period. In this medium period range, the IMs exhibiting best efficiency are *PGV*, *PGD*, *CAD*, V_{rms}, and *I*. The IM number on the horizontal axis corresponds to the number in Table 2. It would be expected that many Class I IMs are largely period dependent. For example, *PGA* (IM #2) exhibits higher efficiency for stiff structures. The period dependence is confirmed by the robustness plot in Figure 2. Only *PGD* (IM #4) shows improved efficiency at higher periods. This would be expected as the maximum displacement approaches the *PGD* in the long period range. The period dependent phenomenon, however, makes any of the Class I IMs a poor choice for an arbitrary structure. Therefore, structure-specific quantities are pursued in the next two sections.

CLASS II INTENSITY MEASURES

Class II and Class III Intensity Measures are both defined as Class I IMs acting on earthquake time histories that have been filtered using different processes. Therefore, the definitions in Table 2 are still valid except u_g (ground motion) has been replaced by u_f (filtered ground motion). Class II IMs are the special case of a single degree of freedom (SDOF) system used as the filter. This is the origin of the traditional spectral quantity *Sd* (spectral displacement). *Sd* is simply the maximum of $u_f(t)$, as defined for *PGD* in Table 2, hence the new notation ^{SDOF}PGD. As there is a large body of research on IMs using this type of filter, there are numerous SDOF specific IMs that are included in this class of IMs in addition to Table 2. These are summarized in Table 3. Note once again the IM numbers are not consecutive between Table 2 and Table 3, but are enumerated following the this table.

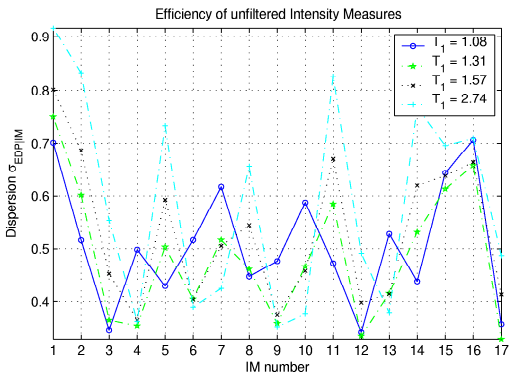

Figure 1 - Efficiency of Class I IMs

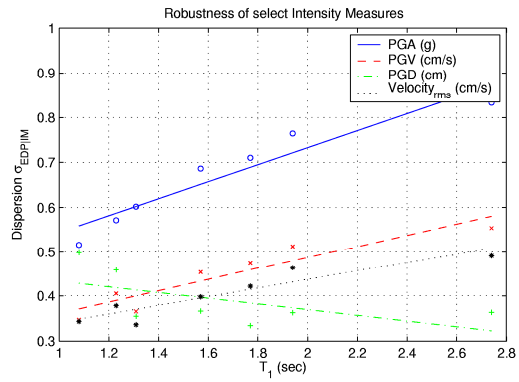

Figure 2 - Robustness of Class I IMs

Table 3 - Class II Intensity Measure Definitions

IM number	IM name	Definition	Units
35	Pseudo-spectral velocity	$PSv(T_i) = \omega_i Sd(T_i)$	cm/s
36	Pseudo-spectral acceleration	$PSa(T_i) = \omega_i^2 Sd(T_i)$	g
54	Luco 1st mode predictor [12]	$IM_{1I} = \lvert PF_1^{[1]} \rvert Sd^I = \frac{Sd^I(T_1,\zeta,d_y)}{Sd(T_1,\zeta)} Sa(T_1,\zeta)$	cm/s2
55	Cordova predictor [13]	$IM_{1eff} = Sa(T_1,\zeta)\left[\frac{Sa(cT_1,\zeta)}{Sa(T_1,\zeta)}\right]^{\alpha}, c = 2, \alpha = \frac{1}{2}$	cm/s2
56	Effective peak acceleration [14]	$EPA = \frac{Sa_{avg}(T_i,\zeta)\Big\rvert_{0.1}^{0.5=T_i}}{2.5}$	g
57	Effective peak velocity	$EPV = \frac{Sv_{avg}(T_i,\zeta)\Big\rvert_{0.7}^{2.0=T_i}}{2.5}$	cm/s
58	Effective peak displacement	$EPD = \frac{Sd_{avg}(T_i,\zeta)\Big\rvert_{2.5}^{4.0=T_i}}{2.5}$	cm
59	Acceleration response intensity [15]	$ASI = \int_{0.1}^{0.5} Sa(T,\zeta=0.05)dT$	g
60	Velocity response intensity	$VSI = \int_{0.7}^{2.0} Sv(T,\zeta=0.05)dT$	cm/s
61	Displacement response intensity	$DSI = \int_{2.5}^{4.0} Sd(T,\zeta=0.05)dT$	cm
62	Response spectrum intensity [16]	$SI = \int_{0.1}^{2.5} Sv(T,\zeta=0.05)dT$	cm
63	Average spectral acceleration	$Sa_{avg} = \sum_{T_1}^{T_n} \frac{Sa(T_i,\zeta)}{n}$	g

64	Average spectral velocity	$Sv_{avg} = \sum_{T_1}^{T_n} \frac{Sv(T_i,\zeta)}{n}$	cm/s
65	Average spectral displacement	$Sd_{avg} = \sum_{T_1}^{T_n} \frac{Sd(T_i,\zeta)}{n}$	cm

The efficiency of all Table 3 IMs is plotted in Figure 3. The IM number on the horizontal axis corresponds to those listed in Table 3. Intermediate values not listed, for example 18 to 34, are simply Class I IMs from Table 2 acting on the SDOF filtered record. Specifically, 18 to 34 are elastic SDOF systems at T_1 and 5% viscous damping, and 37 to 53 are inelastic SDOF systems at T_1, 5% viscous damping, yield strength *fy* of the structure, and 1% strain hardening. IM numbers 63 to 65 (average spectral quantities) are repeated 7 times, each for different period bands about T_1. These are summarized in Table 4.

Table 4 - Average spectral combination IMs

IM number(s)	Name	T_{lower}	T_{upper}
63-65	Band 1	0.5 T_1	2 T_1
66-68	Band 2	4/7 T_1	7/4 T_1
69-71	Band 3	8/13 T_1	13/8 T_1
72-74	Band 4	2/3 T_1	3/2 T_1
75-77	Band 5	8/11 T_1	11/8 T_1
78-80	Band 6	4/5 T_1	5/4 T_1
81-83	Band 7	8/9 T_1	9/8 T_1

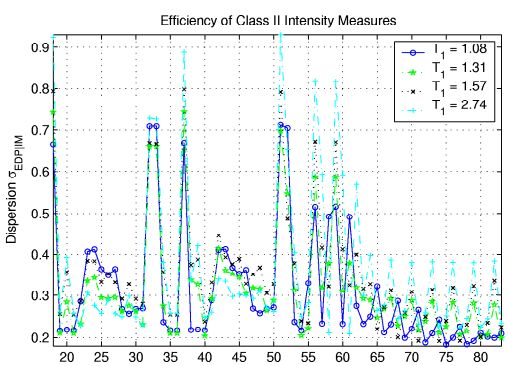

Figure 3 – Efficiency of Class II IMs

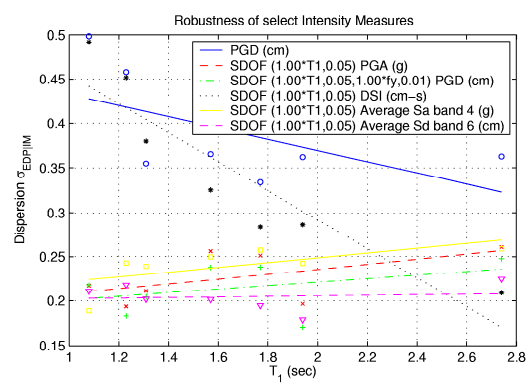

Figure 4 - Robustness of Class II IMs

The most efficient IMs in this class are (filtered SDOF records) elastic ${}^{SDOF}PGA$ (IM #19), elastic pseudo ${}^{SDOF}PGA$ (IM #36), inelastic ${}^{SDOF}PGD$ (IM #40), Luco 1st mode predictor (IM #54), *EPD* (IM #58), *DSI* (IM #61), and the averaged spectral combinations from Table 4. While *DSI* exhibits the lowest dispersion of any IMs for several periods, it is not pursued further due to the large period dependency. It should be considered, however, for long period structures ($T_1 > 2.5$ sec). In most current demand analyses, $Sa(T_1)$ is used as the IM. This is in fact usually the pseudo-spectral acceleration (IM #36), not the actual maximum obtained from differentiating the time history displacement response twice. However, at the low levels of damping considered in this study, and for bridges in general, these quantities are essentially equivalent and only the ${}^{SDOF}PGA$ as defined in Table 2 will be used henceforth (this is the true spectral acceleration).

Given the traditional ${}^{SDOF}PGA$ as a benchmark, it can be seen from Figure 4 that inelastic ${}^{SDOF}PGD$ and averaging *Sa* offer improved efficiency. By narrowing the band around the period of interest, the efficiency of the results continues to improve. However, above band 6, the change in efficiency becomes negligible until it increases back to the level of ${}^{SDOF}PGA$. It should be noticed that all of the IMs from Figure 4 are relatively insensitive to changes in the period. This makes them appealing for use in any structural system. In practical application, the slight improvement in efficiency from using averaged spectral quantities is offset by the large amount of computation required to determine SDOF filtered records at all the intermediate periods. A single inelastic SDOF filtered record achieves similar results and requires only a single analysis.

Although not shown here, the same trends above are true in the transverse direction. However, it should be noted that there is slight negative correlation between period and efficiency in the transverse spectral quantities. This implies shorter period structures would be less efficient, however this was found not to be the general trend [3].

CLASS III INTENSITY MEASURES

Similar to Class II, Class III IMs are Class I IMs acting on filtered time history records. This is a completely general method for viewing IMs, as soon as one realizes the choice of filter is arbitrary and not limited to a SDOF system. This section attempts to introduce several other types of filters that can be used to obtain more efficient demand models. The two primary filters investigated are a more structure-specific application: a two-degree-of-freedom system, and a common signal processing concept: the bandpass filter.

For a structure whose response is dominated by more than just the fundamental mode, it may be beneficial to introduce more information about the second mode into the demand model computation. This can be achieved using a lumped mass and stiffness, two-degree-of-freedom (2DOF) system (Figure 5). For simplicity, it is assumed that each mass in the model is excited equally by the ground motion, and the first mass (m_1) and stiffness values (k_1) are normalized to unity. The remainder of the 2DOF system can be determined with the input of the first and second mode periods, T_1 and T_2. The resulting values for m_2 and k_2 are shown in Equations 3 and 4, respectively.

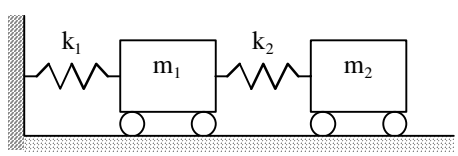

Figure 5 - Two-degree-of-freedom system IM filter

$$m_2 = \frac{-1}{16\pi^4}\left(4\pi^2 - T_1^2\right)\left(4\pi^2 - T_2^2\right) \tag{3}$$

$$k_2 = \frac{1}{T_1^2 T_2^2}\left(-4\pi^2 + T_1^2\right)\left(4\pi^2 - T_2^2\right) \tag{4}$$

In the case of this study, the 2DOF filter is elastic with four input parameters: T_1, T_2, ζ, and u_1 or u_2. The final argument specifies which output record to use as u_f in the subsequent Class I IMs. The damping matrix is formulated using a superposition of modal damping matrices with each of the two modes having damping ratio ζ. Results for efficiency and robustness are shown in Figure 6 and Figure 7, respectively. The IMs with numbers 84 to 100 are Class I IMs acting on the u_1 filtered record; 101 to 117 acting on u_2.

Promising 2DOF filtered IMs include ${}^{2DOF}PGD$ (IM #87), ${}^{2DOF}A_{rms}$ (IM #94), ${}^{2DOF}I_C$ (IM #97), and ${}^{2DOF}I$ (IM #100). The most robust choice is once again ${}^{2DOF}PGD$.

A large amount of computation is required to average spectral quantities from Class II IMs over a range of periods. As shown above, these may be more efficient than spectral quantities at specific periods; therefore, an alternate method of achieving these results is desirable. In signal processing, the bandpass filter is often used to isolate or separate out a range of frequency components from the original source. For this study, a 4th order Butterworth bandpass filter was used with bandwidth B. The bandwidth is the frequency separation between the upper and lower half-power points. The resulting filtered record was then used as u_f in calculating subsequent Class I IMs. Similar to the 2DOF system filter, it is possible to design digital filters of arbitrary cutoff frequencies and frequency bands. Therefore, if desirable, a filter with two or more pass bands could also be used to generate further Class III IMs. This method is considerably more general than developing specific multiple-degree-of-freedom (MDOF) structural models.

The efficiency of Class I IMs acting on bandpass filtered records is shown in Figure 6 (IM numbers 120 to 134). Interestingly, for the bandpass filter, the same IMs are efficient as the 2DOF filter. The highest efficiency is generated by ${}^{BP}I_C$ (IM #131) and ${}^{BP}I_A$ (IM #122); however, this is for the long period range only. The best choice of IM is ${}^{BP}PGA$ (IM #119) for efficiency and robustness. ${}^{BP}I$ (IM #134) is also robust with slightly higher dispersion.

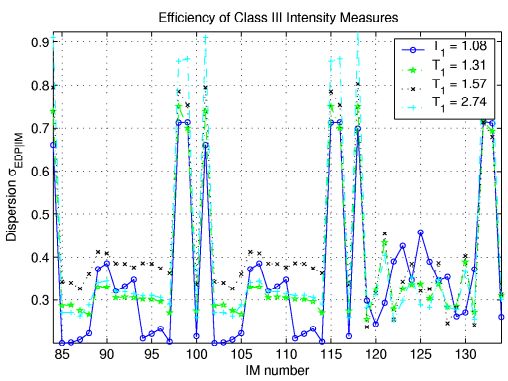

Figure 6 - Efficiency of Class III IMs

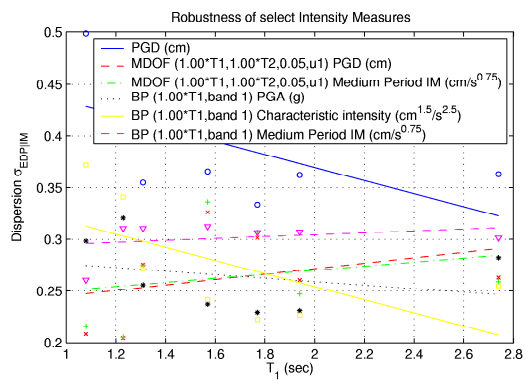

Figure 7 - Robustness of Class III IMs

IM FILTER PARAMETER SENSITIVITY STUDY

With the introduction of filters described for Class II or III IMs comes a choice of filter parameters. All of the filters attempt to improve the predictive qualities of the resulting IMs by incorporating some knowledge of the structure, mainly through structural period. However, numerous other parameters exist and can be tuned to obtain more efficient results. The parameters for Class II are rigorously investigated in the subsection below. Some insight gained is then applied to Class III in the subsequent section.

Class II Parameters

The SDOF system filter has two possible parameters for elastic systems and 4 possible parameters for inelastic systems. The common arguments are period, T, and viscous damping ratio, ζ. The inelastic bilinear system behavior is governed by the yield strength, fy, and the hardening ratio, α. A parametric study of each is explored below.

Period sensitivity

Selection of the fundamental structural period, T_1, is an uncertain proposition by itself. Therefore, basing all Class II and III IMs on this quantity is imposing a lack of knowledge limitation on the resulting PSDMs. The elastic period is largely dependent on the selection of materials and elements in a finite element model or the choice of data sets in empirical period predictions. The elastic period also changes after a structure has experienced inelastic excursions during earthquake excitation. Therefore, this parametric study focuses on the trends in the data to help rationally select a modification factor for filter periods. ${}^{SDOF}PGD$ is selected as the single IM on which to vary parameters as it shows consistently high efficiency.

The sensitivity to period is shown in Figure 8 for the longitudinal direction for the case of three separate structures. The elastic SDOF filter (blue) is contrasted with the inelastic SDOF filter (green) on the same plot. The structures can be identified by the period at the minima from the entries in Table 5. A similar sensitivity plot is shown in Figure 9 for the transverse direction. The selection of a single period at which to develop a SDOF filter appears as a clear minimization problem. Both Figure 8 and Figure 9 are plotted with a fraction of the fundamental period T_1 on the horizontal axis. As mentioned in the introduction, it is necessary to correct these based on the actual lowest period in the direction of interest. This is accomplished (see Table 5) using the pre- and post-gravity load analysis periods in Table 1 and the locations of minima from the above plots (L_{fac} and T_{fac}, or longitudinal factor and transverse factor, respectively).

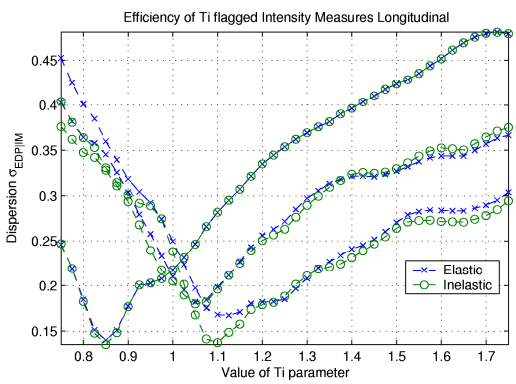

Figure 8 - Longitudinal period sensitivity

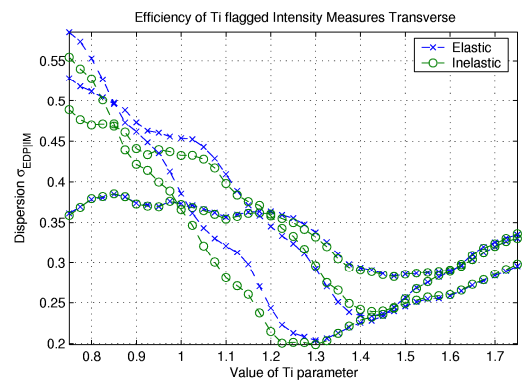

Figure 9 - Transverse period sensitivity

Table 5 - Period modification factors

Structure number	T_{fac} (xT_1)	L_{fac} (xT_1)	L_{fac} (xT_{long})	Post-gravity		Post-eqk.	
				ΔT_{fac}	ΔL_{fac}	ΔT_{fac}	ΔL_{fac}
0001*	1.40	1.12	1.25	0.07	0.21	0.08	0.08
0005*	1.43	1.05	1.20	0.12	0.17	0.07	0.08
0009*	1.23	1.02	1.12	0.10	0.09	0.05	0.27
0013	1.20	1.10	1.19	0.13	0.15	0.04	0.15
0017*	1.30	1.10	1.20	0.07	0.16	0.09	0.09
0021	1.45	0.97	1.22	0.16	0.17	0.16	0.15
0025	1.48	0.85	1.21	0.02	0.18	0.01	0.18

The results indicate the optimal transverse period is $T_T \approx 1.36(T_1)$ and the optimal longitudinal period is $T_L \approx 1.20(T_2)$. T_1 and T_2 in this case refer to the initial elastic periods in the transverse and longitudinal

directions, respectively. Clearly, by choosing the initial elastic period, the single selection of T_1 for Class II IMs would not yield optimal results. It was therefore attempted to relate these period shifts to the loaded condition (post-gravity), a partially damaged condition (post-eqk), and the complete post-earthquake event (displacement ductility EDP). The condition labeled post-eqk is a low-level (elastic) earthquake simulation using the Covina-West Badillo Northridge earthquake record. By applying a ductility demand on the order of 0.5-0.8, cracking and nonlinear concrete behavior is induced, thereby somewhat elongating the period values. Table 5 shows the difference (ΔT_{fac} and ΔL_{fac}) between the observed minima and the post-gravity and post-eqk normalized periods.

For the transverse direction, three predictive equations are proposed for estimating T_{fac} (relative to original T_1, initial elastic period) apriori (Equation 5). The residuals are assumed to be normally distributed with a standard deviation indicated at the end of each equation. The response in the transverse direction is well described by the period after gravity load analysis has been performed. Only to refine the estimate of T_{fac} (designated T_{fac}^*), would it be necessary to incorporate information about the expected displacement ductility demand.

$$T_{fac}^* = \begin{cases} T_{fac,gravity} & \sigma = 0.11 \\ T_{fac,eqk} & \sigma = 0.09 \\ 0.325\sqrt{\mu_\Delta} + 0.741 T_{fac,gravity} & \sigma = 0.07 \end{cases} \tag{5}$$

For the longitudinal direction, the results differ somewhat. The post-gravity load analysis period gives a poor estimate of L_{fac} (relative to original T_2, initial elastic period), however, the expected displacement ductility demand and post-earthquake period are better predictors (Equation 6). To reduce the scatter in the prediction, the post-gravity load factor is combined with the average displacement ductility demand to better estimate L_{fac} (designated L_{fac}^*).

$$L_{fac}^* = \begin{cases} \sqrt{\mu_\Delta} & \sigma = 0.20 \\ L_{fac,eqk} & \sigma = 0.17 \\ \sqrt{\mu_{\Delta,mean}} L_{fac,gravity} & \sigma = 0.04 \end{cases} \tag{6}$$

The displacement ductility demands (μ_Δ) used in the analyses are the mean plus half standard deviation for each given structure, unless otherwise noted.

Damping coefficient sensitivity

Almost all spectral analyses done today use a damping coefficient of 5% of critical. This may not agree with the damping in any of the actual structural modes under consideration. The finite element model of the bridge uses Rayleigh damping calculated for the first two modes. The specified damping ratio was 2.5% of critical. Using the calculated α_1 and β_2 parameters (mass and stiffness proportional damping), the effective damping ratio in each of the modes could be back calculated. For both the longitudinal and transverse directions, this value was 2.6% for both pre- and post-gravity load analysis. These values were then also verified by free vibration tests on the structure in each of these directions. This indicated whether other modes were present in the two primary directions. Free vibration results yielded similar damping values, 2.3% for the longitudinal direction, and 3.1% for the transverse direction. Transverse free vibration did include a small contribution from the 3rd mode, especially for structures 0021 and 0025 (Table 1).

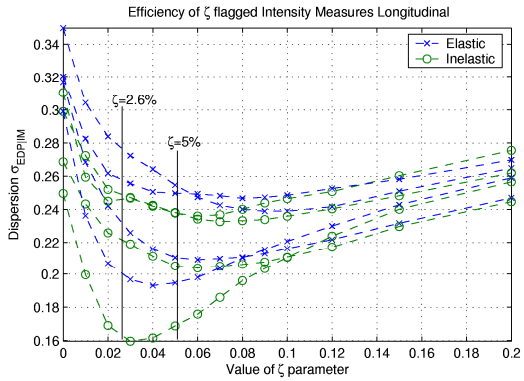

Figure 10 - Longitudinal ζ sensitivity

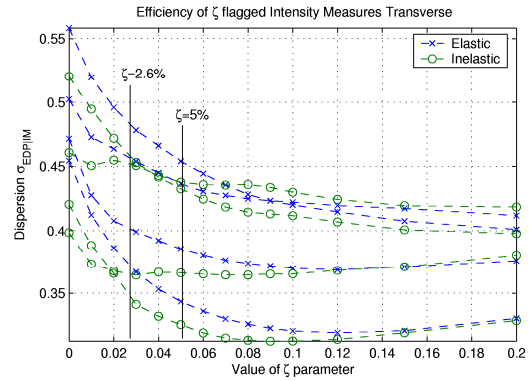

Figure 11 - Transverse ζ sensitivity

Figure 10 shows the sensitivity to damping ratio in the longitudinal direction, Figure 11 in the transverse direction for structures marked with an asterix in Table 5. There are no apparent trends in either direction that suggest an improved value of the damping ratio to use in SDOF filters. While not the optimal value, the use of 5% damping in each case yields better results than using the system damping ratio.

Yield strength sensitivity

For the case of the inelastic SDOF filter, the yield strength of the system needs to be specified as an additional parameter. A bilinear fit to the nonlinear force-displacement pushover response of the structure is made. The yield strength is chosen to minimize the area between the pushover curve and bilinear approximation (eg. FEMA [17]). While there appears to be some benefit to allowing the onset of hysteretic behavior (lower *fy*), there is no definitive optimal choice of this parameter (Figure 12). The values on the abscissa are normalized with respect to the selected yield strength of the system. It should also be noted that selection of *fy* from a nonlinear pushover is not exact, but given the bounds on the *fy* parameter in this study, it would suggest the exact value chosen is unimportant.

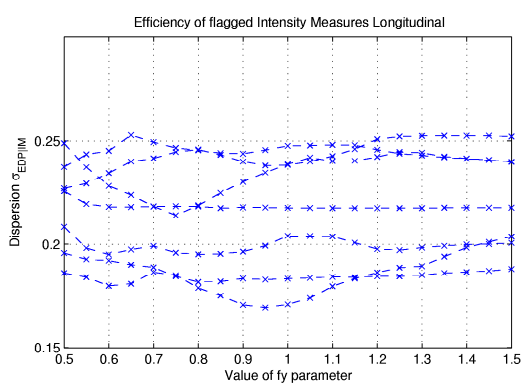

Figure 12 - Longitudinal *fy* sensitivity

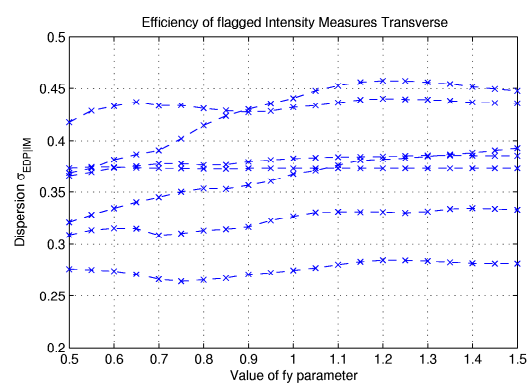

Figure 13 - Transverse *fy* sensitivity

Hardening ratio sensitivity

The hardening ratio can be determined from the bilinear fit made to the pushover of the structure. Only the sensitivity to the hardening ratio in the longitudinal direction is shown (Figure 14). The value can be varied widely and have little impact on the model efficiency. A value of 0.02 is recommended for use with inelastic SDOF filters. It should be noted the value used for steel strain hardening in the finite element model was 1.5%. Transverse results are comparable and not shown here.

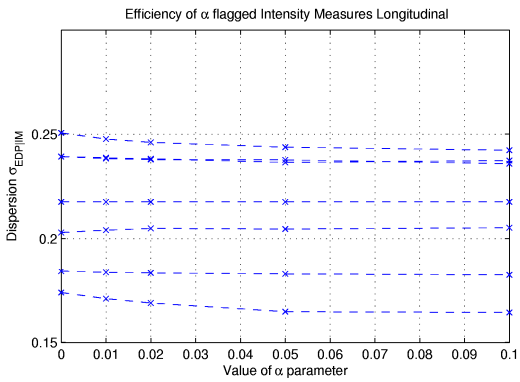

Figure 14 - Longitudinal α sensitivity

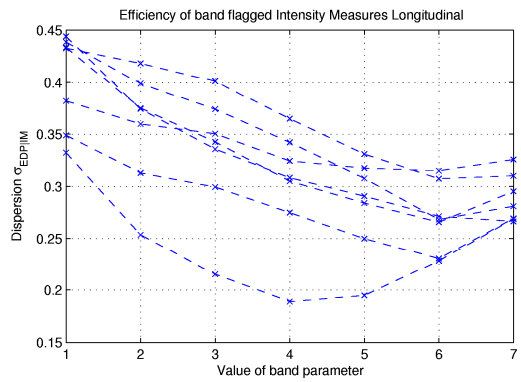

Figure 15 - Longitudinal band sensitivity

Class III Parameters

Focusing on the 2DOF filter introduced earlier, the individual values of T_1 and T_2 were not varied explicitly, nor with respect to each other. However, the relationships developed for the SDOF filter periods (T_{fac}* and L_{fac}* in Equations 5 and 6, respectively) were applied to the 2DOF filter to determine if this was beneficial to the efficiency of the 2DOF filter as well. Compared to the values for the basic MDOF filter in Figure 6, the selection of optimal SDOF periods also slightly improves the overall performance for the 2DOF filter.

Focusing on the bandpass filter, a parameter study was performed using the same procedure as for the SDOF filter. It was assumed that the optimal single period, and therefore the central frequency, was determined using Equations 5 and 6. The only parameter that was varied was then the bandwidth B of the filter. The same values were used as in Table 4 to facilitate comparison. A comparison of results is shown for the bandpass filter and the corresponding averaged spectral combinations in Figure 15. As with the average spectral quantities from Table 4, choosing a bandwidth between bands 5 and 6 produces optimal results.

CONCLUSIONS

Several thousand existing and new IMs were considered in this exhaustive study. The goal was to develop a probabilistic seismic demand model that exhibited a high level of efficiency. This allows a higher level of confidence in achieving performance objectives, both at the demand level, and as part of a performance-based earthquake engineering framework. It was not intended to achieve increased efficiency by developing spectral or other combinations with calibrated structure-specific constants. Rather, from the existing pool of IM knowledge, it was intended to isolate the input parameters that make IMs better predictors in PSDMs. By choosing a medium and long period range of bridge structures with which to generate these models, the period dependence (lack of robustness) of Class I (unfiltered) IMs was revealed. This facilitated the optimal selection of parameters for Class II (SDOF filtered) IMs and possible future development of new Class III (arbitrary filter) IMs.

While current use of $Sa(T_1)$ as the IM in seismic performance assessment provides better efficiency than previously used IMs such as PGA, $Sa(T_1)$ is neither the best IM choice, nor is T_1 the best period choice. It was determined that inelastic ${}^{SDOF}PGD$ outperforms elastic ${}^{SDOF}PGD$ (standard spectral displacement) for a large period range. Depending on the direction of concern (longitudinal or transverse), a modified period value outperforms the initial elastic period. By performing gravity load analysis, or low-level static

or dynamic analysis on the structure, the resulting period is a better predictor for post-earthquake response. It is also possible to modify the initial elastic period by the expected displacement ductility demand on the structure during the earthquake. Equations 5 and 6 can be used to accomplish this period modification. For the inelastic SDOF filter, the yield strength obtained from the nonlinear pushover response should be used. The hardening ratio corresponding to the global structural hardening ratio should be employed, and a damping ratio of 5% of critical selected.

If improved efficiency above ${}^{SDOF}PGD$ is desired, this quantity should be averaged over a narrow band (0.8 to 1.25 times period) around the filter's structural period. To be more computationally efficient, this procedure can also be accomplished using a bandpass filter with the same frequency band. For a structure with earthquake response in several modes, the concept of a MDOF or multiple pass band Class III filter can be investigated.

ACKNOWLEDGEMENTS

This work was supported in part by the Earthquake Engineering Research Centers Program of the National Science Foundation under award number EEC-9701568 through the Pacific Earthquake Engineering Research Center (PEER). Any opinions, findings, and conclusions or recommendations expressed in this material are those of the author(s) and do not necessarily reflect those of the National Science Foundation.

REFERENCES

1. Krawinkler H. "A general approach to seismic performance assessment." Proceedings of the International Conference on Advances and New Challenges in Earthquake Engineering Research, Hong Kong, August 19-20, 2002.
2. Cornell CA, Krawinkler H. "Progress and challenges in seismic performance assessment." PEER Center News 2000; 3(2).
3. Mackie K, Stojadinovic B. "Seismic demands for performance-based design of bridges." PEER Report. Submitted for publication, 2003.
4. Cornell CA, Jalayer F, Hamburger RO, Foutch DA. "Probabilistic basis for 2000 SAC/FEMA steel moment frame guidelines." Journal of Structural Engineering 2002; 128(4): 526-533.
5. Shome N, Cornell CA. "Probabilistic seismic demand analysis of nonlinear structures." Reliability of Marine Structures Report No. RMS-35. Stanford: Department of Civil and Environmental Engineering, Stanford University, 1999.
6. Mackie K, Stojadinovic B. "Probabilistic seismic demand model for California highway bridges." Journal of Bridge Engineering 2001; 6(6): 468-481.
7. Caltrans. "Seismic Design Criteria 1.1." Sacramento: California Department of Transportation, 1999.
8. Conte JP. "Ground motion intensity measures for performance-based earthquake engineering." Proceedings of Applications of Statistics and Probability in Civil Engineering. 2003.
9. Joyner WB, Boore DM. "Measurement, characterization, and prediction of strong ground motion." Earthquake Engineering and Soil Dynamics II – Recent advances in ground motion evaluation. New York: ASCE, 1988: 43-102.
10. Arias A. "A measure of earthquake intensity." RJ Hansen, Editor. Seismic design for nuclear power plants. Cambridge: MIT Press, 1970: 438-483.
11. Fajfar P. "A measure of earthquake motions capacity to damage medium period structures." Soil Dynamics and Earthquake Engineering 1990.
12. Luco N, Cornell CA. "Structure-specific scalar intensity measures for near-source and ordinary earthquake ground motions." Earthquake Spectra.

13. Cordova PP. "Development of a two-parameter seismic intensity measure and probabilistic seismic assessment procedure." PEER Report 2000/10. Berkeley: Pacific Earthquake Engineering Research Center, University of California Berkeley, 2000:.
14. ATC. "Tentative provisions for the development of seismic regulations for buildings." ATC 3-06. Palo Alto: Applied Technology Council, 1978.
15. Von Thun JL, Rochim LH, Scott GA, Wilson JA. "Earthquake ground motions for design and analysis of dams." Earthquake Engineering and Soil Dynamics II – Recent advances in ground motion evaluation. New York: ASCE, 1988: 463-481.
16. Housner GW. "Behavior of structures during earthquakes." Journal of Engineering Mechanics Division; 85(EM14): 109-129.
17. Federal Emergency Management Agency. "Seismic rehabilitation prestandard." Report No. FEMA-356. Washington DC: FEMA, 2002.
18. Giovenale, P. "Comparison of ground motion intensity measures using the IDA." Proceedings of Applications of Statistics and Probability in Civil engineering, 2003.
19. Sucuoglu, H. "Influence of ground motion intensity parameters on elastic response spectra." Proceedings of the 11th European Conference on Earthquake Engineering, 1998.